Progress In Electromagnetics Research, Vol. 120, 235–247, 2011

BROADBAND AND HIGH-GAIN PLANAR VIVALDI ANTENNAS BASED ON INHOMOGENEOUS ANISOTROPIC ZERO-INDEX METAMATERIALS

B. Zhou, H. Li, X. Y. Zou, and T. J. Cui*

State Key Laboratory of Millimeter Waves, School of Information Science and Engineering, Southeast University, Nanjing 210096, China

Abstract—Vivaldi antennas have broad applications in real practice due to the ultra wideband properties. However, their gain and directivity are relatively low. In this paper, a new method is presented to improve the gain and directivity of Vivaldi antennas in a broad band using inhomogeneous and anisotropic (IA) zero-index metamaterials (ZIM). ZIM have the ability to enhance the antenna directivity; anisotropic ZIM with only one component of the permittivity or permeability tensor approaching to zero can make impedance match to improve the radiation efficiency; and IA-ZIM can broaden the frequency bandwidth. Single- and multiple-layered planar IA-ZIM have been analyzed, designed, and fabricated, which can be embedded into the original Vivaldi antenna smoothly and compactly. The IA-ZIM-based Vivaldi antennas have good features of high gain, high directivity, low return loss, and broad bandwidth. Compared to the original Vivaldi antenna, the measurement results show that the gain has been increased by 3 dB and the half-power beam width has been decreased by 20 degrees with the reflection coefficient less than −10 dB from 9.5 GHz to 12.5 GHz after using IA-ZIM.

1. INTRODUCTION

Vivaldi antenna which was first proposed by Gibson in 1979 [1] has broad applications in many fields, such as in the imaging system [2], the communication system, the ultra- wideband system [3], etc., due to its convenient-integrated, easy-fabricated, and portable characteristics. However, the directivity of Vivaldi antenna is relatively low. Recently,

Received 27 July 2011, Accepted 29 August 2011, Scheduled 6 September 2011

* Corresponding author: Tie-Jun Cui (tjcui@seu.edu.cn).

some improvement methods have been proposed, such as to use the photonic bandgap (PBG) substrate [4], the array technique, etc. But such methods are very complicated, expensive, and have large volumes. With the development of metamaterials, some other innovative and effective methods have been introduced into antennas to improve their directivity [5–8]. Zero-index of refraction is such a feasible way and has attracted much attention. However, the former zero-index metamaterials (ZIM) had poor radiation efficiency due to the impedance mismatch when the permittivity or permeability approaches to zero [9, 10]. More recently, the anisotropic ZIM with one component of the permittivity or permeability tensor close to zero have been presented to solve the problem [11, 12]. Different from isotropic ZIM, the impedance of anisotropic ZIM along the wave-propagation direction can be designed to match with that of background. Hence, high antenna efficiency can be achieved using the anisotropic ZIM, which has been reported in our former work recently [13]. However, the bandwidth of ZIM and anisotropic ZIM is narrow due to the resonant nature.

In this paper, we propose a concept of inhomogeneous and anisotropic (IA) ZIM, which maintain the advantages of high gain and high radiation efficiency of the anisotropic ZIM but increase the bandwidth. We have presented the analysis, design, and fabrication of single- and multiple-layered planar IA-ZIM, which can be embedded into the original Vivaldi antenna smoothly and compactly. Based on the IA-ZIM, new types of Vivaldi antennas have been fabricated and measured, which possess high gain, high directivity, low return loss, and broad bandwidth. Compared to the original Vivaldi antenna, the measurement results show that the gain has been increased by 3 dB and the half-power beam width has been decreased by 20 degrees with the reflection coefficient less than -10 dB from 9.5 GHz to 12.5 GHz after using IA-ZIM. Hence the new antennas have great potentials in real applications.

2. DESIGNS OF ANISOTROPIC ZIM AND VIVALDI ANTENNA

2.1. Unit Cell Design of Anisotropic ZIM

The choice of metamaterial unit cell is essential to the whole device. The meander-line resonator [14] was used in our design and experiments, as shown in Fig. 1. For the consideration of anisotropic metamaterials, different polarizations are imposed and analyzed. The electric field in Fig. 1(a) is along the x direction, while in Fig. 1(b) is along the y direction.

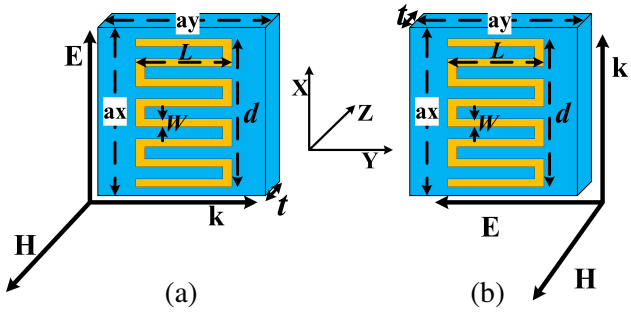

Figure 1. The designed unit cell of the meander-line structure on a dielectric substrate, in which $ax = ay = 4\,\text{mm}$, $W = 0.2\,\text{mm}$, $d = 3.77\,\text{mm}$, $L = 2.7\,\text{mm}$, $t = 0.5\,\text{mm}$, and the dielectric substrate is chosen as F4B with the permittivity of 2.65 and the tangent loss of 0.001. The meander-line structure was placed symmetrically. Both cell models have the same parameters, however, with different incident waves. (a) The electric polarization is along the x direction. (b) The electric polarization is along the y direction.

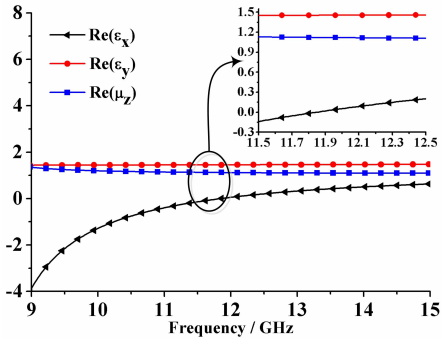

Figure 2. The retrieved results of the metamaterial unit cell when $L = 2.1\,\text{mm}$. As the value of L changes, similar results are obtained. Additionally, ε_y and μ_z are approximately equal to ensure the impedance matching to free space.

After making full-wave simulations of the unit cell using the commercial Software (CST Microwave Studio) followed by the standard retrieval procedure [15], we get the retrieved results of the effective medium parameters when L is equal to 2.1 mm, as shown in Fig. 2. As the arm length (L) of the meander-line changes, a shift of the zero-permittivity points can be observed. When L equals 2.1 mm, 2.4 mm, and 2.7 mm, the operating frequency is at around 10 GHz, 10.8 GHz,

and 11.85 GHz, respectively. This is the basic principle of the proposed inhomogeneous ZIM.

2.2. The Geometry of Vivaldi Antenna

The design of Vivaldi antenna is a complicated task due to its multiple parameters. The geometry in our design is shown in Fig. 3, and the detailed values of such parameters are listed in Table 1. The opening taper curve is determined by the following equation

$$y = C_1 e^{\alpha x} + C_2$$

where α is the rate of opening,and C_1 and C_2 can be calculated by the start and end points P_1 and P_2:

$$C_1 = \frac{y_2 - y_1}{e^{\alpha x_2} - e^{\alpha x_1}} \qquad C_2 = \frac{y_1 e^{\alpha x_2} - y_2 e^{\alpha x_1}}{e^{\alpha x_2} - e^{\alpha x_1}}$$

The substrate of the Vivaldi antenna is the same as the former used for the metamaterial unit cell. Furthermore, both of them have the same thickness for easy integration. The antenna is fed by a 50 microstrip line, which has a width of 1.3 mm. A broadband method consisting of a circular cavity at the slot line and a radial stub at the microstrip line was introduced. The impedances of microstrip line and slot line at the crossing area are matched to reduce the reflection. After the optimization of such parameters, an ultra broadband from 2.5 GHz to 13 GHz can be achieved.

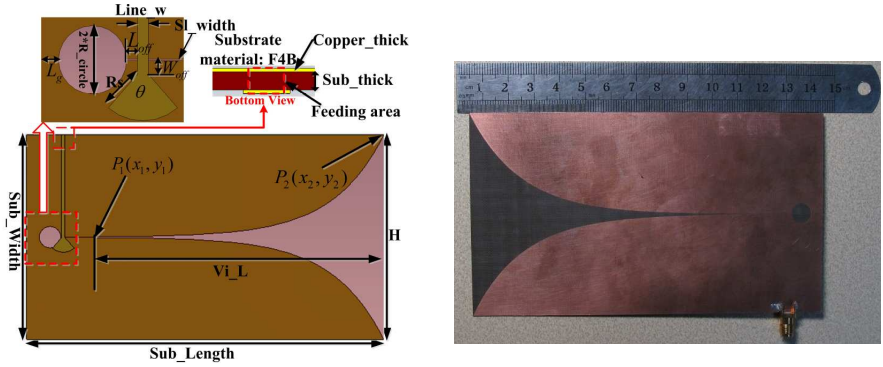

Figure 3. The simulation model and the fabricated sample of the original Vivaldi antenna. (a) The antenna model and the geometrical parameters. (b) The fabricated sample.

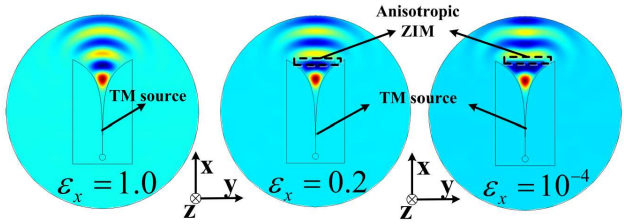

(a)

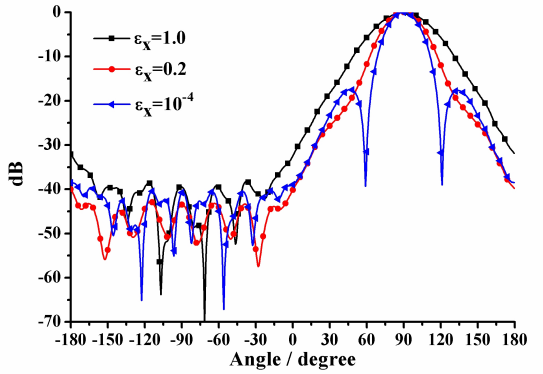

(b)

Figure 4. Simulation results of the traditional Vivaldi antenna with and without the anisotropic ZIM lens ($\varepsilon_x = 1.0$, $\varepsilon_x = 0.2$ and $\varepsilon_x = 10^{-4}$) at 10 GHz. (a) The near-field distributions. (b) The far-field radiation patterns.

Table 1. The detailed parameters of the Vivaldi antenna.

Sub_Width	Sub_Length	Sub_thick	Vi_L	Line_w
80 mm	140 mm	0.5 mm	120 mm	1.3 mm
H	L_g	R_circle	R_s	Copper_thick
80 mm	5 mm	4.2 mm	7 mm	0.018 mm
Sl_width	L_{off}	W_{off}	θ	α
0.12 mm	1 mm	−0.6 mm	82°	0.05

3. PRINCIPLE ANALYSES AND DESIGN OF BROADBAND AND HIGH-GAIN VIVALDI ANTENNAS

Based on the commercial software (COMSOL MultiPhysics), the impact of an anisotropic ZIM lens which is placed in front of the Vivaldi antenna on the antenna performance is observed, as illustrated in Fig. 4. Near the point of zero permittivity, the value of permittivity is very small, which can also improve the antenna performance.

In our simulations, a TM line source (along the z axis) is used to generate the TM wave propagating along the x direction, with the magnetic field polarized along the z axis, as shown in Fig. 4. In the anisotropic ZIM lens, the x component of the permittivity either approaches to zero ($\varepsilon_x = 10^{-4}$) or is small ($\varepsilon_x = 0.2$), while the y component is equal to 1 ($\varepsilon_y = 1$). From the simulation results, we observe that the directivity of the TM wave is greatly improved, as shown in Fig. 4(a). When is smaller, the improvement becomes significant. This can be clearly seen from the far-field radiation patterns illustrated in Fig. 4(b).

The above phenomena can be explained from the EM theory. For easy implementation, we consider the wave propagation in homogeneous anisotropic ZIM. The dispersion relation for TM polarization is written as

$$\frac{k_x^2}{\varepsilon_y} + \frac{k_y^2}{\varepsilon_x} = \frac{\omega^2}{c^2}\mu_z$$

in which ε_x, ε_y, μ_z are components of the permittivity and permeability tensors. When $\varepsilon_x \to 0$, $\varepsilon_y \neq 0$, $\mu_z \neq 0$, it can be derived that $k_y \to 0$, which indicates that no waves (or very few waves) will propagate along the y direction. Hence the propagation constant along the x direction equals

$$k_x = \frac{\omega}{c}\sqrt{\varepsilon_y \mu_z}$$

and the corresponding wave impedance is

$$\eta_x = \eta_0\sqrt{\mu_z/\varepsilon_y}$$

If ε_y and μ_z are approximately equal, the wave impedance will match to that of free space. On the other hand, from the Maxwell equations, we obtain

$$\frac{\partial H_z}{\partial y} = -i\omega\varepsilon_x E_x$$

Since $\varepsilon_x \to 0$, H_z should be constant with respect to y. The above analysis can predict the wave propagation inside the homogenous

anisotropic ZIM lens approximately, as shown in Fig. 3(a). According to the boundary condition, outside the ZIM lens, the EM fields will keep such distributions near the boundary, generating high directivity to the x direction.

More importantly, since the anisotropic metamaterial has few contributions to the loss of wave propagation along the x direction due to the above-analyzed impedance match, it is attractive to use different-size unit cells working at different zero-index points along the propagation direction to extend the frequency bandwidth. Through the same process as shown in Fig. 2, we obtain the retrieved curves for ε_x with different arm lengths of the mean-line (L), as demonstrated in Fig. 5. If we focus the region with the absolute value of ε_x below 0.2 to approximate ZIM, then the unit cells with $L = 2.1$ mm cover the frequency range from 9.55 GHz to 10.55 GHz; the unit cells with $L = 2.4$ mm cover the frequency range from 10.45 GHz to 11.45 GHz; while unit cells with $L = 2.7$ mm cover the frequency range from 11.35 GHz to 12.5 GHz. Hence the inhomogeneous anisotropic ZIM composed of such three kinds of unit cells will have a broad bandwidth from 9.55 GHz to 12.5 GHz.

With the combination of the original Vivaldi antenna and the anisotropic ZIM, we propose broadband and high-gain Vivaldi antennas. Fig. 6(a) illustrates the design of the antenna, which is based on the original planar Vivaldi antenna by printing ZIM structures on its opening taper area. To broaden the bandwidth of the anisotropic ZIM, three kinds of unit cells demonstrated earlier are used to construct

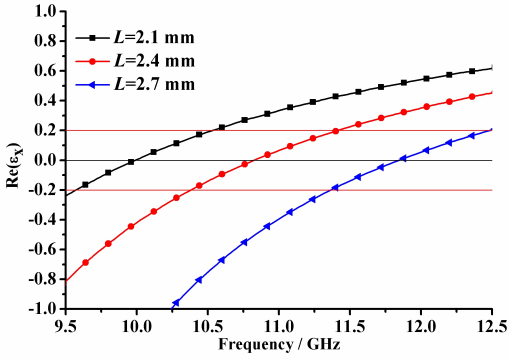

Figure 5. The retrieved results of the metamaterial unit cells with different arm lengths. The shift of zero-index points is clearly observed. If we focus the region with the absolute value of below 0.2, a broad frequency band from 9.5 GHz to 12.5 GHz can be obtained.

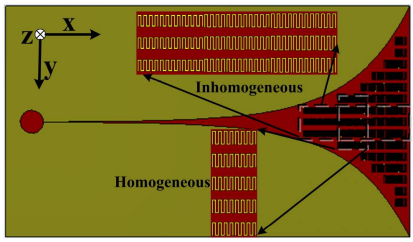

(a)

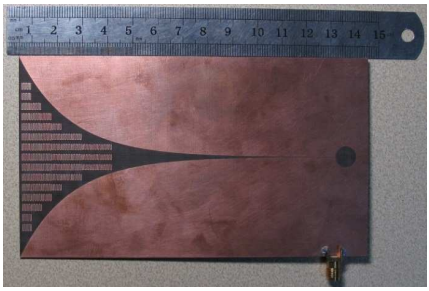

(b)

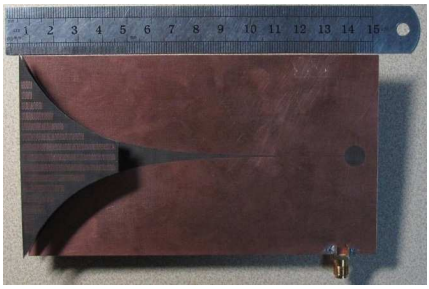

(c)

Figure 6. The designed and fabricated Vivaldi antennas with IA-ZIM. (a) The simulation model with single-layer IA-ZIM. (b) The fabricated sample of the Vivaldi antenna with single-layer IA-ZIM. (c) The fabricated sample of the Vivaldi antenna with multi-layers IA-ZIM.

inhomogeneous anisotropic ZIM on the main path of the antenna, as shown in Fig. 6(a). Along the main path which directly connects to the feeding source, three cascaded sections of anisotropic ZIM are designed: the first section is realized using the unit cells with $L = 2.1\,\text{mm}$; the second section is realized using the unit cells with $L = 2.4\,\text{mm}$; and the third with $L = 2.7\,\text{mm}$. In other regions on the opening area, which are less important for the wave propagation than the main path, homogeneous anisotropic ZIM structures with $L = 2.4\,\text{mm}$ are utilized, as shown in Fig. 6(a). It is expected that the proposed antenna has a broad bandwidth from 9.5 GHz to 12.5 GHz with high gains.

The designed antenna has been fabricated, as demonstrated in Fig. 6(b). Since the anisotropic ZIM structures are directly printed on the original Vivaldi antenna (single-layer PCB), this is called as the Vivaldi antenna with single-layer IA-ZIM. Comparing Figs. 3(b) and 6(b), we clearly notice that the new antenna does not bring any additional burden (size, volume, and weight) with respect to the

original Vivaldi antenna. In order to improve the antenna performance and make the anisotropic ZIM more like a lens, we designed and fabricated multi-layer ZIM, as shown in Fig. 6(c). A foam with the height of 3 mm was used to connect the adjacent layers. Apparently, this is still a planar structure with multiple layers, bringing a little additional burden on the hight and weight of the antenna.

4. EXPERIMENTAL RESULTS

In experiments, the aim is to verify the enhancement to the gain and directivity of the original Vivaldi antenna shown in Fig. 3(b) in the designed bandwidth (from 9.5 GHz to 12.5 GHz) using single- and multiple-layered IA-ZIM depicted in Figs. 6(b) and (c). Experimental results have demontrated that IA-ZIM can greatly improve the performance of the Vivaldi antenna in a broad band. Fig. 7(a) illustrates the reflection coefficients, or the insertion losses, of the three antennas. It is clearly observed that the use of IA-ZIM does not destroy the extra-wideband property of the original Vivaldi antenna. In an extra broad bandwidth from 2.5 GHz to 13.5 GHz, the reflection coefficients of three antennas are all below -10 dB.

However, the gain and directivity (in E-plane) of the Vivaldi antenna are significantly improved after using IA-ZIM, as illustrated in Figs. 7(b)–(f). In the region of approximate anisotropic ZIM from 9.5 GHz to 12.5 GHz, we notice that the gain of the new Vivaldi antenna increases by around 2 dB while the half-power beam width (HPBW) decreases by around 15 degrees using the single-layer IA-ZIM, compared to the original Vivaldi antenna. With the aid of multi-layered IA-ZIM, more significant performance is achieved: the gain increases by around 4dB while the HPBW decreases by around 25 degrees. Table 2 gives the detailed performance comparison between the original and new Vivaldi antennas.

From above measurement results, we conclude that the use of IA-ZIM does improve the antenna's performance in the designed IA-ZIM frequency band. In the rest of the bandwidth, however, we do not hope the antenna's performance becomes worse. Fig. 8 illustrates the measured gains of original Vivaldi antenna and IA-ZIM-based antennas over the whole frequency band, from which we clearly observe that the antenna's gain has also been improved in most regions. Only in a small region of low frequencies, the antenna's gain is maintained or slightly deteriorated, as shown in Fig. 8.

The H-plane radiation patterns of three antennas are also considered to judge the antenna's overall performance. The measured results of the H-plane radiation patterns are plotted in Fig. 9. Clearly,

the use of IA-ZIM has a small influence on the H-plane patterns, but the influence is not significant at all to keep the main features of antennas, as shown in Fig. 9. As a consequence, the proposed IA-ZIM design can be applied to improve the overall performance of the Vivaldi antenna in a broad bandwidth.

Comparing to a recent work on the compact UWB antipodal Vivaldi antenna [16], the IA-ZIM technique provides better capability

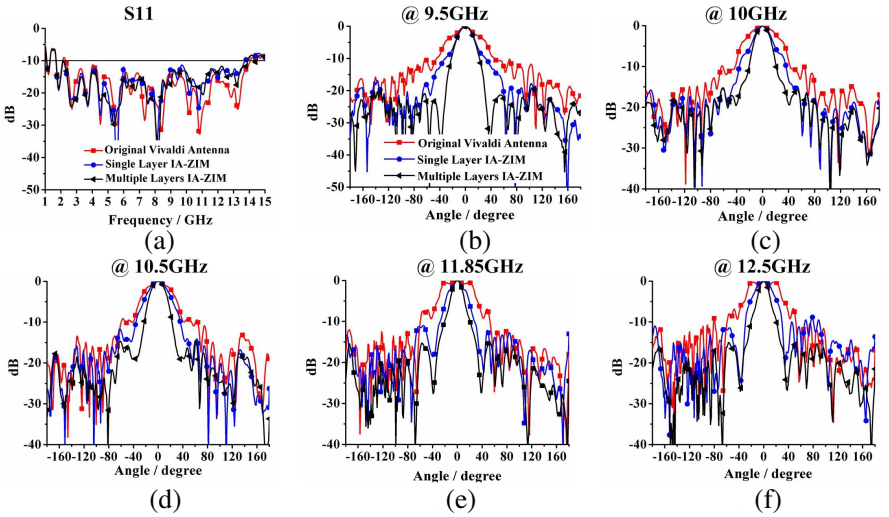

Figure 7. The measurement results of the original and IA-ZIM-based Vivaldi antennas. (a) The reflection coefficient (S_{11}). (b) The E-plane radiation patterns at 9.5 GHz. (c) The E-plane radiation patterns at 10 GHz. (d) The E-plane radiation patterns at 10.5 GHz. (e) The E-plane radiation patterns at 11.85 GHz. (f) The E-plane radiation patterns at 12.5 GHz.

Table 2. The measured HPBW of the original and IA-ZIM-based Vivaldi antenna.

Antenna Type	@ 9.5 GHz	@ 10 GHz	@ 10.5 GHz	@ 11.85 GHz	@ 12.5 GHz
Original	40.5°	48.4°	48.7°	55.8°	54.6°
Single layer	24°	27°	36°	26.6°	29.2°
Multiple layers	24°	23.2°	26°	18°	17.6°

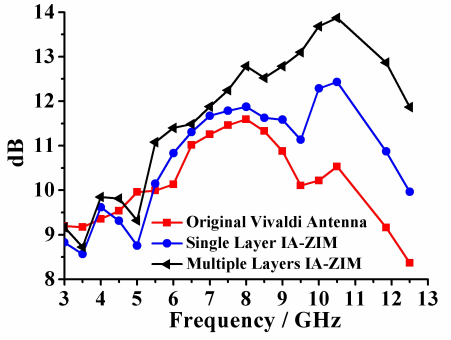

Figure 8. The measured gain across the whole band from 3 GHz to 12.5 GHz.

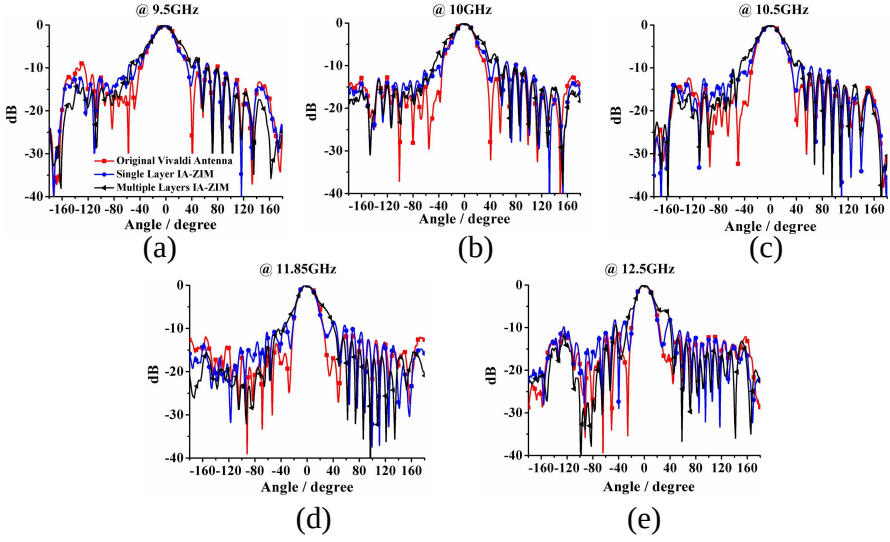

Figure 9. The measurement resutls of H-plane radiation patterns, (a) at 9.5 GHz, (b) at 10 GHz, (c) at 10.5 GHz, (d) at 11.85 GHz, (e) at 12.5 GHz.

(up to 4-dB higher gain) in the designed frequency band. To improve the antenna's performance in other frequency bands, we only need to adjust the arm-length of metamaterial unit cells. The proposed IA-ZIM method can also be applied to the antennas reported in Ref. [16] to further improve the performance, because the IA-ZIM method is not conflicting to the optimization method used in Ref. [16].

5. CONCLUSION

In this work, we have proposed single-layer and multi-layer IA-ZIM which are incorporated efficiently to the traditional Vivaldi antenna to improve the gain and directivity in a broad bandwidth. Experimental results show that both the directivity and gain can be enhanced significantly from 9.5 GHz to 12.5 GHz by using IA-ZIM. It is more important that ZIM can be embedded into the original Vivaldi antenna very easily and smoothly, and do not increase additional volume burdens and costs. Hence the new Vivaldi antenna can be applied in practical applications.

ACKNOWLEDGMENT

This work is supported in part by a Major Project of the National Science Foundation of China under Grant Nos. 60990320 and 60990324, in part by the 111 Project under Grant No. 111-2-05, and in part by the National Science Foundation of China under Grant Nos. 60871016, 60901011, and 60921063.

REFERENCES

1. Gibson, P. J., "The Vivaldi aerial," *Proc. 9th Eur. Microwave Conf.*, No. 1, 101–105, 1979.
2. Chiappe, M. and G. Gragnani, "Vivaldi antennas for microwave imaging: Theoretical analysis and design considerations," *IEEE Transactions on Instrumentation and Measurement*, Vol. 55, No. 2, 1885–1891, 2006.
3. Schantz, H., "Introduction to ultra-wideband antennas," *IEEE Conference on Ultra Wideband Systems and Technologies*, No. 3, 1–9, 2003.
4. Ellis, T. J. and G. M. Rebeiz, "MM-wave tapered slot antennas on micromachined photonic bandgap dielectrics," *IEEE MTT-S Int. Microwave Symp. Dig.*, No. 4, 1157–1160, 1996.
5. Lovat, G., et al., "Analysis of directive radiation from a line source in a metamaterial slab with low permittivity," *IEEE Transactions on Antennas and Propagation*, Vol. 54, No. 5, 1017–1030, 2006.
6. Zhou, H., et al., "A novel high-directivity microstrip patch antenna based on zero-index metamaterial," *IEEE Antennas and Wireless Propagation Letters*, Vol. 8, No. 6, 538–541, 2009.
7. Wu, B.-I., W. Wang, J. Pacheco, X. Chen, T. M. Grzegorczyk, and J. A. Kong, "A study of using metamaterials as antenna substrate

to enhance gain," *Progress In Electromagnetics Research*, Vol. 51, No. 5, 295–328, 2005.

8. Yang, R., Y.-J. Xie, P. Wang, and L. Li, "Microstrip antennas with left-handed materials substrates," *Journal of Electromagnetic Waves and Applications*, Vol. 20, No. 9, 1221–1233, 2006.
9. Oraizi, H., A. Abdolali, and N. Vaseghi, "Application of double zero metamaterials as radar absorbing materials for the reduction of radar cross section," *Progress In Electromagnetics Research*, Vol. 101, 323–337, 2010.
10. Wang, B. and K. Huang, "Shaping the radiation pattern with mu and epsilon-near-zero metamaterials," *Progress In Electromagnetics Research*, Vol. 106, 107–119, 2010.
11. Ma, Y., et al., "Near-field plane-wave-like beam emitting antenna fabricated by anisotropic metamaterial," *Applied Physics Letters*, Vol. 94, No. 7, 2009.
12. Cheng, Q., et al., "Radiation of planar electromagnetic waves by a line source in anisotropic metamaterials," *Journal of Physics D: Applied Physics*, Vol. 43, No. 8, 35406, 2010.
13. Zhou, B. and T. J. Cui, "Directivity enhancement to Vivaldi antennas using compactly anisotropic zero-index metamaterials," *IEEE Antennas and Wireless Propagation Letters*, Vol. 10, No. 9, 2011.
14. Tang, W. X., H. Zhao, X. Zhou, J. Y. Chin, and T.-J. Cui, "Negative index material composed of meander line and SRRs," *Progress In Electromagnetics Research B*, Vol. 8, 103–114, 2008.
15. Smith, D., et al., "Determination of effective permittivity and permeability of metamaterials from reflection and transmission coefficients," *Physical Review B*, Vol. 65, No. 11, 195104, 2002.
16. Bai, J., S. Shi, and D. W. Prather, "Modified compact antipodal Vivaldi antenna for 4–50-GHz UWB application," *IEEE Trans. Microwave Theory Tech.*, Vol. 59, No. 12, 1051–1057, 2011.